FULL PAPER

Dalton
www.rsc.org/dalton

Reactions of $[W_2(OCH_2{}^tBu)_8]$ (M=M) with diazobenzene and trimethylsilyldiazomethane. Preparation and structures of $W_2(OCH_2{}^tBu)_8(NPh)$ and $W_2(OCH_2{}^tBu)_8(N_2C(H)SiMe_3)$

Malcolm H. Chisholm,* Damon R. Click, Judith C. Gallucci and Christopher M. Hadad
Department of Chemistry, The Ohio State University, 100 W. 18th Avenue, Columbus, Ohio 43210, USA. E-mail: chisholm@chemistry.ohio-state.edu

Received 25th April 2003, Accepted 6th June 2003
First published as an Advance Article on the web 15th July 2003

Hydrocarbon solutions of $W_2(OCH_2{}^tBu)_8$ (M=M) react with azobenzene at room temperature to give the phenylimido-bridged compound $W_2(\mu\text{-NPh})(\mu\text{-}OCH_2{}^tBu)_2(OCH_2{}^tBu)_6$ which has a confacial biooctahedral geometry with a W–W single bond length of 2.5613(2) Å and W–N = 1.987(3) Å (ave). Similarly, $W_2(OCH_2{}^tBu)_8$ (M=M) and trimethylsilyldiazomethane react to give the 1 : 1 adduct $W_2(\mu\text{-}N_2C(H)SiMe_3)(\mu\text{-}OCH_2{}^tBu)_2(OCH_2{}^tBu)_6$ which has a W–W distance of 2.5626(2) Å and W–N = 1.985(1) Å (ave). The $\mu\text{-}N_2CHSiMe_3$ ligand can be described as a hydrazonido(2−) ligand. The N–N distance is 1.366(4) Å and the N–N–C angle is 120.1(3)°. The NNC plane of the bridging ligand is perpendicular to the W–W bond axis. The bonding in these molecules is discussed in the light of electronic structure calculations employing density functional theory. The present findings are contrasted with related reactions involving MM multiply bonded compounds and with low valent early transition metal complexes that are similarly known to activate N–N bonds.

In contrast to the extensive reaction chemistry of the MM triple bond complexes, those having MM double bonds have been little studied.[1] In part, this may reflect upon two factors. 1) There are relatively few complexes having MM double bonds and 2) of those that are known, many are coordinatively saturated involving face or edge sharing biooctahedra as seen in the solid state structure of MoO_2.[2] Although the compound $[W_2(OCH_2{}^tBu)_8]$ is believed to adopt a similar structure in the solid state,[3] it reacts as though it were coordinatively unsaturated and can ligate such molecules as carbon monoxide, ethyne, ethylene, allene and acetone.[4] It is also reactive to the Group 16 elements forming the series $W_2(\mu\text{-E})(\mu\text{-}OCH_2{}^tBu)_2(OCH_2{}^tBu)_6$ where E = O, S, Se and Te.[5] This reaction represents the formal conversion of a MM double bond to a MM single bond by a two-electron redox process. We thus became interested in the reactions between $[W_2(OCH_2{}^tBu)_8]$ and azobenzene which might, by a double bond metathesis reaction, lead to $PhNW(OCH_2{}^tBu)_4$ or some other product of addition. Compounds of the type $ArNW(OR)_4$ are well known,[6] and earlier work by Cotton had shown a similar metathesis reaction involving a NbNb double bond.[7] Also, the direct addition of molecular O_2 to $[W_2(OCH_2{}^tBu)_8]$ gives $OW(OCH_2{}^tBu)_4$.[4] Similarly diazoalkanes are known to add to some MM bonded complexes,[8] and, in other cases, eliminate N_2 and yield carbenes. We have previously shown that $[W_2(\mu\text{-}CH_2)(\mu\text{-}OCH_2{}^tBu)_2(OCH_2{}^tBu)_6]$ is formed in the reaction between $[W_2(OCH_2{}^tBu)_8]$ and $Ph_3P{=}CH_2$,[4] while $M_2(OR)_6$ (M=M) compounds (M = Mo or W) react with diazoalkanes to give products of oxidative-addition and reduction of the diazo ligand.[8d] This prompted us to investigate the reaction between $[W_2(OCH_2{}^tBu)_8]$ and Me_3SiCHN_2. We describe herein the results of our studies of these two reactions.

Results and discussion

Syntheses

a $W_2(\mu\text{-NPh})(\mu\text{-}OCH_2{}^tBu)_2(OCH_2{}^tBu)_6$. $[W_2(OCH_2{}^tBu)_8]$ reacts with azobenzene in hydrocarbon solvents at 50 °C over 24 hours to give the red phenylimido compound $W_2(NPh)(OCH_2{}^tBu)_8$ which can be crystallized at low temperatures from concentrated hydrocarbon solution. This phenylimido compound is formed when $[W_2(OCH_2{}^tBu)_8]$ was allowed to react with 0.5, 1.0 and 5.0 equiv. of azobenzene. It is inert to the presence of excess azobenzene at 50 °C. However, in all reactions, a trace of a colorless crystalline compound was formed. We were not able to collect sufficient of this to characterize it, but we consider it is quite probably $PhNW(OCH_2{}^tBu)_4$ which is akin to the known $ArNW(OR)_4$ compounds[6] and, in this reaction, may be formed by a competitive kinetic pathway.

b $[W_2(\mu\text{-}N_2CHSiMe_3)(\mu\text{-}OCH_2{}^tBu)_2(OCH_2{}^tBu)_6$. $[W_2(OCH_2{}^tBu)_8]$ and trimethylsilyldiazomethane (1 equiv.) react in hydrocarbon solvents at 25 °C to yield the 1 : 1 adduct as a red crystalline solid upon crystallization from cold hexanes solutions. This compound is inert with respect to further reaction with Me_3SiCHN_2 at this temperature.

Spectroscopic characterization data

Both compounds are diamagnetic and yield ^{1}H NMR spectra consistent with their solid-state structures (*vide infra*) in which there are confacial biooctahedra with two bridging alkoxides and one nitrogen-containing bridging ligand. In solution, these approximate C_{2v} symmetry and the RO groups give rise to three singlets arising from the ^{t}Bu groups in the ratio 4 : 2 : 2. The methylene protons appear as two singlets of relative intensity 4 : 4 and an AB quartet of intensity 8. The singlets arise from the methylene protons associated with the bridging neopentoxide groups and those that are *trans* to the bridging nitrogen atom. These all lie on a mirror plane. The methylene protons on the other four alkoxide ligands are diastereotopic. The phenylimido ligand shows the expected signals for a C_6H_5 moiety while the diazoalkane group has a methine proton signal at δ 8.54 and a methine carbon signal at 166.5 ppm consistent with an "sp^2-like" carbon atom.

The electronic absorption spectra of the diazoalkane and phenylimido compound show intense absorption in the UV region of the spectrum which tails into the visible. This low energy shoulder at $\lambda_{max} \approx 500$ nm is relatively weak ($\varepsilon \approx 300$ M^{-1} cm^{-1}) and is assignable to a MM based electronic transition while, for the diazoalkane complex, the absorption centered at 260 nm, which shows a vibronic progression ($\nu \approx 1000$ cm^{-1}), is associated with a N lp to π^* transition of the bridging ligand. See Fig. 1.

Solid state and molecular structures

$W_2(NPh)(OCH_2{}^tBu)_8$. An ORTEP drawing of the phenylimido complex is shown in Fig. 2. There is a central confacial

DOI: 10.1039/b304587k

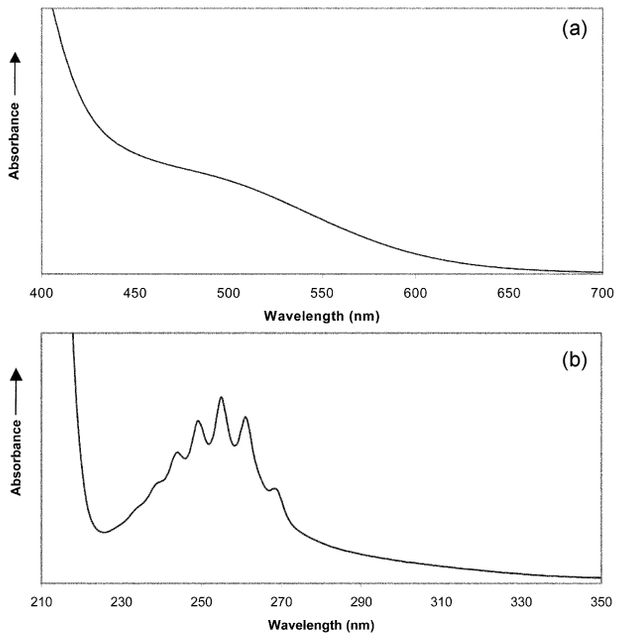

Fig. 1 Electronic absorption spectrum of $W_2(\mu\text{-}N_2C(H)SiMe_3)$-$(\mu\text{-}OCH_2{}^tBu)_2(OCH_2{}^tBu)_6$ in the 350–210 nm range (bottom), and 400–700 nm (top), recorded as a THF solution at 25 °C.

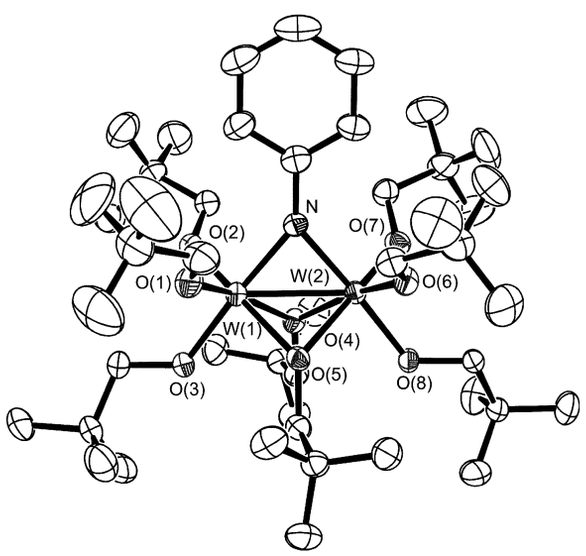

Fig. 2 ORTEP[24] drawing of the $W_2(\mu\text{-}NPh)(\mu\text{-}OCH_2{}^tBu)_2(OCH_2{}^tBu)_6$ molecule. Thermal ellipsoids are drawn at the 50% probability level.

biooctahedral $O_3WO_2NWO_3$ unit with a W–W separation of 2.5613(2) Å, consistent with a MM single bond. The sum of the angles at nitrogen are 360° consistent with sp^2 hybridization. The W–O distances of the bridging ligands are notably longer than those of the terminal alkoxides as would be expected: 2.087–2.091(2) *vs.* 1.878–1.952(2) Å. The short W–N distances, together with the trigonal nitrogen atom, implies that the nitrogen p orbital that is perpendicular to the W_2N plane is intimately involved in π-bonding. Selected bond distances and bond angles are given in Table 1.

$W_2(N_2CHSiMe_3)(OCH_2{}^tBu)_8$. An ORTEP drawing of the diazoalkane adduct is given in Fig. 3. This drawing gives the atom number scheme and emphasizes the similarity of the confacial biooctahedral $O_3WNO_2WO_3$ moiety. Selected bond distances and angles are given in Table 2. The metric parameters of this central unit are remarkably similar to those of the imido complex leading to the view that the diazoalkane ligand can be considered as a dianionic ligand and that the ditungsten center

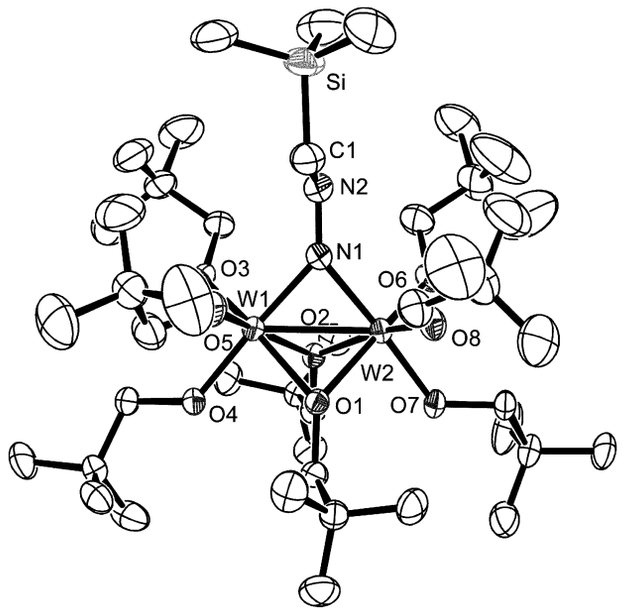

Fig. 3 ORTEP drawing for the $W_2(\mu\text{-}N_2C(H)SiMe_3)(\mu\text{-}OCH_2{}^tBu)_2$-$(OCH_2{}^tBu)_6$ molecule. Thermal ellipsoids are drawn at the 50% probability level.

has been oxidized and now has a W–W single bond. The W–N distances are similar to those in the phenylimido complex and the nitrogen bonded to each tungsten is essentially planar, with 358.7° as the sum of the angles about N1. The W–O distances follow a similar pattern implying again that the bridging nitrogen ligands have a higher *trans*-influence than the alkoxides.

A view of the diazoalkane complex looking down the WW bond axis is given in Fig. 4. This view shows that the bridging diazoalkane ligand is distinctly angular with NNC and NCSi angles of 120.1(3) and 121.2(3)°, respectively. This, together with the N–N distance, 1.366(4) Å, and N–C = 1.266(5) Å indicate that the bridging ligand is best considered as a hydrazonido(2−) ligand.

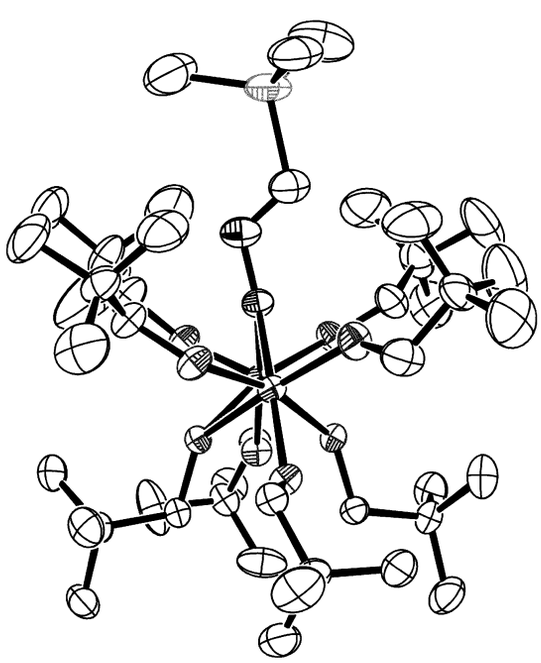

Fig. 4 ORTEP drawing for the molecule $W_2(\mu\text{-}N_2C(H)SiMe_3)$-$(\mu\text{-}OCH_2{}^tBu)_2(OCH_2{}^tBu)_6$ looking down the W–W axis. This view of the molecule clearly emphasizes the confacial central $O_3WO_2NWO_3$ skeleton and the angular geometry of the NNC group of the bridging diazoalkane ligand. Thermal ellipsoids are drawn at the 50% probability level.

Table 1 Selected experimental and calculated bond distances (Å) and angles (°) for $W_2(\mu\text{-NPh})(\mu\text{-OCH}_2{}^t\text{Bu})_2(\text{OCH}_2{}^t\text{Bu})_6$ and $W_2(\mu\text{-NPh})(\mu\text{-OCH}_3)_2(\text{OCH}_3)_6$ molecules, respectively

W(1)–W(2)	Exp.	2.5613(2)	W(2)–N	Exp.	1.987(3)
	Calc.	2.61		Calc.	2.03
W(1)–N	Exp.	1.987(3)	W(2)–O(4)	Exp.	2.088(2)
	Calc.	2.03		Calc.	2.12
W(1)–O(1)	Exp.	1.878(2)	W(2)–O(5)	Exp.	2.090(2)
	Calc.	1.92		Calc.	2.12
W(1)–O(2)	Exp.	1.887(2)	W(2)–O(6)	Exp.	1.889(3)
	Calc.	1.92		Calc.	1.92
W(1)–O(3)	Exp.	1.946(2)	W(2)–O(7)	Exp.	1.883(3)
	Calc.	1.97		Calc.	1.92
W(1)–O(4)	Exp.	2.087(2)	W(2)–O(8)	Exp.	1.952(2)
	Calc.	2.12		Calc.	1.97
W(1)–O(5)	Exp.	2.091(2)	N–C(1)	Exp.	1.418(5)
	Calc.	2.12		Calc.	1.39

W(1)–N–W(2)	Exp.	80.3(1)	N–W(2)–O(8)	Exp.	176.4(1)
	Calc.	79.9		Calc.	174.6
W(1)–N–C(1)	Exp.	139.3(3)	W(1)–O(4)–W(2)	Exp.	75.7(1)
	Calc.	140.2		Calc.	76.1
W(2)–N–C(1)	Exp.	140.5(3)	W(2)–O(5)–W(1)	Exp.	75.6(1)
	Calc.	139.9		Calc.	76.1
N–W(1)–O(3)	Exp.	176.7(1)			
	Calc.	174.7			

Table 2 Selected experimental and calculated bond distances (Å) and angles (°) for $W_2(\mu\text{-N}_2\text{C(H)SiMe}_3)(\mu\text{-OCH}_2{}^t\text{Bu})_2(\text{OCH}_2{}^t\text{Bu})_6$. The calculations were performed on the model complex $W_2(\mu\text{-N}_2\text{C(H)SiMe}_3)(\mu\text{-OCH}_3)_2(\text{OCH}_3)_6$

W(1)–W(2)	Exp.	2.5626(2)	W(2)–N(1)	Exp.	1.986(3)
	Calc.	2.62		Calc.	2.03
W(1)–N(1)	Exp.	1.984(2)	W(2)–O(1)	Exp.	2.099(2)
	Calc.	2.03		Calc.	2.12
W(1)–O(1)	Exp.	2.082(2)	W(2)–O(2)	Exp.	2.094(2)
	Calc.	2.12		Calc.	2.12
W(1)–O(2)	Exp.	2.100(2)	W(2)–O(6)	Exp.	1.884(2)
	Calc.	2.12		Calc.	1.91
W(1)–O(3)	Exp.	1.889(2)	W(2)–O(7)	Exp.	1.939(2)
	Calc.	1.91		Calc.	1.97
W(1)–O(4)	Exp.	1.941(2)	W(2)–O(8)	Exp.	1.882(2)
	Calc.	1.97		Calc.	1.92
W(1)–O(5)	Exp.	1.889(2)	N(2)–C(1)	Exp.	1.266(5)
	Calc.	1.92		Calc.	1.29
N(1)–N(2)	Exp.	1.366(4)			
	Calc.	1.35			

W1)–N(1)–W(2)	Exp.	80.4(1)	N(2)–C(1)–Si	Exp.	121.2(3)
	Calc.	80.3		Calc.	119.8
N(1)–W(1)–O(4)	Exp.	176.9(1)	W(1)–N(1)–N(2)	Exp.	137.5(2)
	Calc.	172.2		Calc.	138.5
N(1)–N(2)–C(1)	Exp.	120.1(3)	W(2)–N(1)–N(2)	Exp.	140.8(2)
	Calc.	121.3		Calc.	138.7
N(1)–W(2)–O(7)	Exp.	174.8(1)			
	Calc.	172.3			

Electronic structure and bonding

In order to examine the bonding in the imido and diazoalkane complexes, we have undertaken electronic structure calculations employing density functional theory with the aid of the Gaussian 98 suite of programs (See Experimental section). In both cases, the neopentoxide ligands were modeled with methoxide and the starting geometry of $W_2(OCH_3)_8(\mu\text{-bridge})$ was taken from the crystal structure and allowed to optimize in C_1 symmetry. A comparison of the calculated and observed bond distances for the central core of the two molecules is given in Tables 1 and 2. The calculation consistently overestimates the W–W, W–N and W–O bond distances though the trends are consistent with those observed. A similar finding was observed for the calculations performed on the series $W_2(\mu\text{-E})(OCH_3)_8$ in relation to the experimental $W_2(\mu\text{-E})(OCH_2{}^t\text{Bu})_8$, where E = O, S, Se and Te.[5] It is, however, fair to state that the calculations are consistent with the existence of a M–M single bond and either a bridging phenylimido or hydrazonido(2−) ligand.

The frontier orbitals for the phenylimido compound are shown in Fig. 5. The HOMO is the M–M σ orbital comprised mostly of W d_{z^2} atomic orbitals. The HOMO − 1 is mostly bridge centered having some Np to Wd character (a metal π/d combination), and considerable phenyl π character. The orientation of the C_5 ring allows for maximum overlap with the Np_π orbital and, in the HOMO, this interaction is antibonding. The LUMO is comprised of an in-phase combination of two metal hybrid π/δ type orbitals that are out-of-phase in regards to the in-phase π-combination of the N and C(*ipso*) carbon p_π orbitals. The LUMO + 1 is mainly an out-of-phase combination of two metal π/δ hybrids.

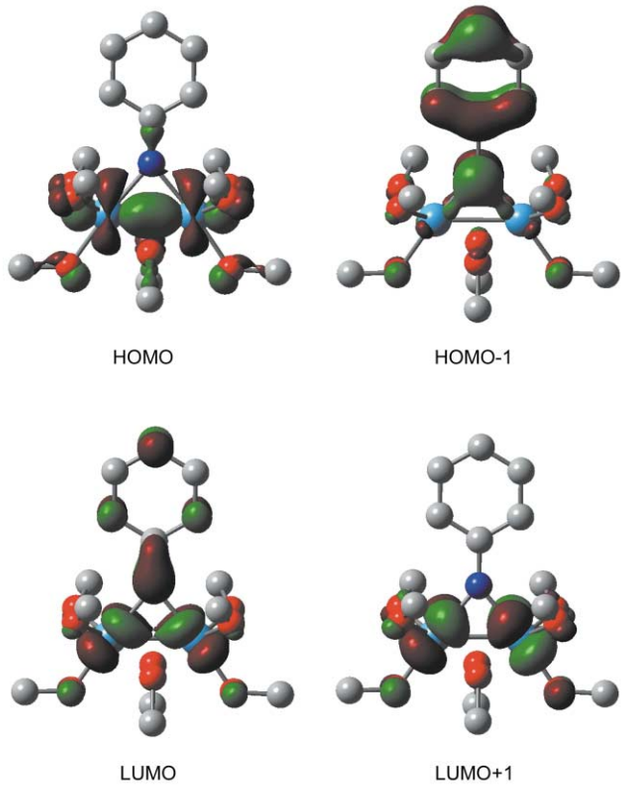

Fig. 5 Plots of the frontier molecular orbitals of $W_2(\mu\text{-NPh})(\mu\text{-OCH}_3)_2(OCH_3)_6$.

The frontier molecular orbitals for the diazoalkane adduct are shown in Fig. 6. The HOMO is predominantly M–M σ bonding which is comprised of overlap of the tungsten d_{z^2} orbitals. The HOMO − 1 orbital is p_π lone-pair based that is essentially non-bonding with respect to the dinuclear center. The HOMO − 2 orbital is comprised of an N lone-pair orbital that is parallel with respect to the metal–metal bond and this MO is also C=N π bonding. The LUMO is comprised of an out-of-phase combination of two metal hybrid π/δ type orbitals that are out-of-phase in regard to the terminal oxygen p_π orbitals. The LUMO + 1 is an in-phase combination of two metal hybrid π/δ type orbitals which are out-of-phase with respect to terminal oxygen p_π orbitals. The LUMO + 2 orbital is an in-phase combination of two metal hybrid π/δ type orbtials that are out-of-phase with respect to four terminal oxygen p_π orbitals and the two bridging oxygen p_π orbitals. In comparison, for the related complex $W_2(\mu\text{-NPh})(\mu\text{-OCH}_2{}^t\text{Bu})_2(OCH_2{}^t\text{Bu})_6$, the HOMO is predominantly M–M σ bonding which is comprised of the tungsten's d_{z^2} orbitals. The HOMO − 1 orbital is comprised of an out-of-plane N p_π orbital that is bonding in a π-type fashion with the in-phase combination of two metal hybrid π/δ type orbitals. Furthermore, the phenyl ring has a bonding and anti-bonding combination with one node and the out-of-plane N p_π orbital is anti-bonding with regard to this combination. The LUMO is comprised of an in-phase combination of two metal hybrid π/δ type orbitals that are out-of-phase in regard to an in-phase π combination of the N and C(*ipso*) orbitals. The LUMO + 1 is mainly an out-of-phase combination of two metal hybrid π/δ type orbitals.

Comparisons with related chemistry

Given the propensity of the elements molybdenum and tungsten to bind nitrogen and to form M–N multiple bonds, it is not surprising to find that earlier studies of the reactions between diazoalkanes and dinuclear compounds with M–M triple bonds, specifically $Cp_2Mo_2(CO)_4$ and $M_2(OR)_6$ were also found to give diazoalkane adducts, both bridging and terminal.[8] In

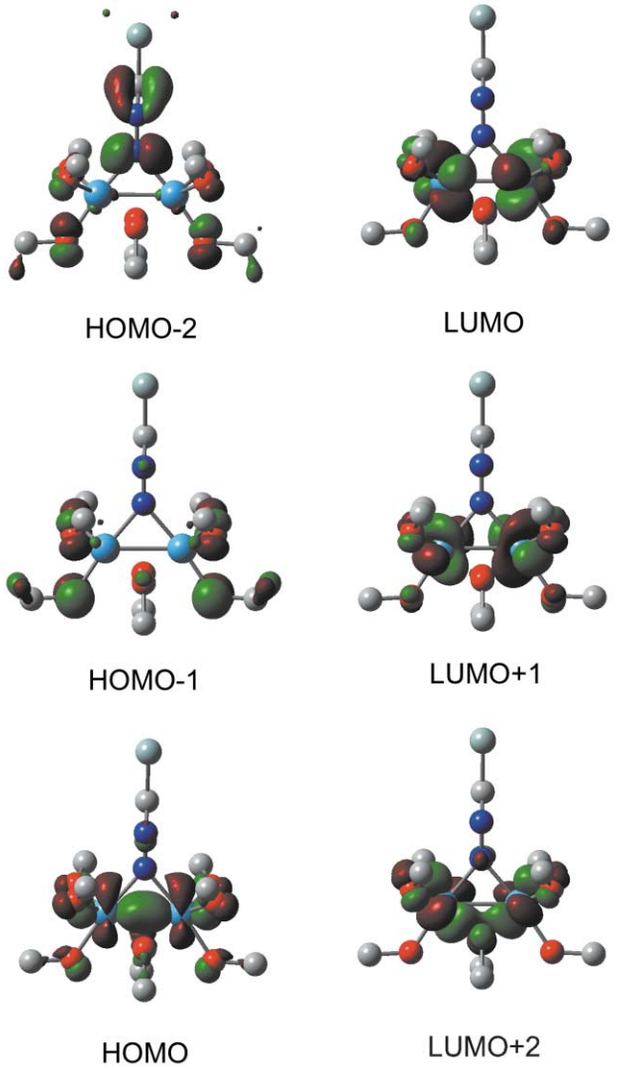

Fig. 6 GaussView plots of the frontier molecular orbitals of $W_2(\mu\text{-N}_2\text{-C(H)SiMe}_3)(OCH_3)_8$.

contrast, the reactions of M–M double bonded complexes $[(\eta^5\text{-}C_5R_5)M(CO)_2]_2$, where M = Co, Rh, Ir and R = H, Me, gave bridging alkylidene complexes with elimination of dinitrogen.[9]

In the chemistry of diazobenzene, Cotton and co-workers were the first to report the cleavage of the N–N double bond in a reaction with a Nb–Nb double bonded complex: $[NbCl_2(SMe_2)]_2(\mu\text{-Cl})_2(\mu\text{-SMe}) + PhNNPh \longrightarrow [NbCl_2(SMe_2)(NPh)]_2(\mu\text{-Cl})_2$.[7] Reactions of the MM triply-bonded complexes $M_2(OR)_6$ (M = Mo, W) were also found to reductively cleave azobenzene and, more recently, Floriani working with M–M double bonded complexes of niobium and molybdenum supported by calixarene ligands reported four electron reductions of diazobenzene to phenylimido-niobium(V) and -molybdenum(VI) complexes.[10] With mononuclear tungsten(II) arlyoxides, Rothwell has also seen the four-electron reduction to give $(ArO)_2W(NPh)_2$ compounds.[11] In main group element chemistry, addition is often seen across an element–element double bond as in the addition of Me_3SiCHN_2 to [Ge=Ge].[12]

Given these findings of others, our results are interesting but not exceptional. It is, however, noteworthy that in the reactions of $[W_2(OCH_2{}^t\text{Bu})_8]$, the reaction stops at the 2-electron redox stage. The reactions proceed to convert d^2–d^2 M–M double bonded compounds to d^1–d^1 M–M single bonded ones, and the latter are inert to further oxidation to give $(RO)_4W$(VI)-imido or -hydrazonido compounds, despite the fact that the latter are known and may be prepared by alternate routes. It seems likely that the tungsten(VI) complexes are indeed the thermodynamic products and, in this instance, the d^1–d^1 dinuclear compounds

are the kinetic products. It also seems likely that the first step in the reaction is adduct formation to give a compound of the type $(RO)_3W(\mu\text{-}OR)_3W(OR)_2L$ where L = η^1-PhNNPh or $N_2CH\text{-}SiMe_3$. Then a redox reaction and terminal bridge exchange leads to the observed bridged imido or hydrazonido complexes. Further speculation at this time is not warranted.

Experimental

All manipulations were carried out under an inert atmosphere of oxygen-free UHP-grade argon using standard Schlenk techniques or under a dry and oxygen-free atmosphere of nitrogen in a Vacuum Atmospheres Co. Dry Lab System. Hexane was degassed and distilled from potassium under nitrogen. Toluene-d_8 was degassed, stirred over sodium for 24 h and vacuum transferred to an ampoule. Azobenzene and trimethylsilyldiazomethane were purchased form Aldrich and used as received. NMR spectra were recorded on a 400 MHz Bruker DPX Avance^{400} spectrometer. All ^{1}H NMR chemical shifts are reported in ppm relative to the ^{1}H impurity in toluene-d_8 at δ 2.09. $[W_2(OCH_2{}^tBu)_8]_n$ was prepared according to literature procedures.[3]

Preparation of $W_2(\mu\text{-}NPh)(\mu\text{-}OCH_2{}^tBu)_2(OCH_2{}^tBu)_6$

To a 25 mL round-bottomed flask was added $[W_2(OCH_2{}^tBu)_8]_n$ (0.100 g, 0.094 mmol) and PhNNPh (9.5 mg, 0.094 mmol). Hexanes (10 mL) were added to give a purple slurry and the reaction was heated to 50 °C. After stirring for 24 h, the solution was filtered through a medium glass frit with a Celite pad. Stripping the solvent gave a red solid identified as $W_2(\mu\text{-}NPh)(\mu\text{-}OCH_2{}^tBu)_2(OCH_2{}^tBu)_6$ in 95% crude yield. X-Ray quality crystals were obtained upon crystallization from hexanes at −20 °C. ^{1}H NMR (400 MHz, toluene-d_8, 27 °C): δ 0.98 (s, 36 H), 1.02 (s, 18 H), 1.24 (s, 18 H), 4.22 (d, 4 H, J_{H-H} = 10 Hz), 4.36 (d, 4 H, J_{H-H} = 10 Hz), 4.63 (s, 4 H), 4.83 (s, 4 H), 7–8 (m, Ph). ^{13}C{^{1}H} NMR (100 MHz, toluene-d_8, 27 °C): δ 26.72 (s, $C(CH_3)_3$), 27.70 (s, $C(CH_3)_3$), 28.00 (s, $C(CH_3)_3$), 33.85 (s, CH_2), 34.26 (s, CH_2), 34.90 (s, CH_2), 81.30 (s, $C(CH_3)_3$, 83.12 (s, $C(CH_3)_3$, 85.09 (s, $C(CH_3)_3$, 120–140 (Ph). Anal. Calc. for $W_2O_8NC_{46}H_{93}$: C, 47.77; H, 8.10; N, 1.27 Found: C, 47.25; H, 8.01; N, 1.25%.

Preparation of $W_2(\mu\text{-}NNC(H)SiMe_3)(\mu\text{-}OCH_2{}^tBu)_2(OCH_2{}^tBu)_6$

To a 25 mL round-bottomed flask was added $[W_2(OCH_2{}^tBu)_8]_n$ (0.100 g, 0.094 mmol). Hexanes (10 mL) were added to give a purple slurry and the solution was cooled to −30 °C. $NNC(H)SiMe_3$ (37.5 μL, 0.094 mmol).was added by syringe and the reaction was allowed to warm to room temperature. After stirring for 24 h the solution was filtered through a medium glass frit with a Celite pad. Stripping the solvent gave a red solid identified as $W_2(\mu\text{-}NNC(H)SiMe_3)(\mu\text{-}OCH_2{}^tBu)_2(OCH_2{}^tBu)_6$ in 95% crude yield. X-Ray quality crystals were obtained upon crystallization from hexanes at −20 °C. ^{1}H NMR (400 MHz, toluene-d_8, 27 °C): δ 0.33 (s, 9 H), 0.99 (s, 36 H), 1.02 (s, 18 H), 1.21 (s, 18 H), 4.38 (d, 4 H, J_{H-H} = 11 Hz), 4.52 (s, 4 H), 4.71 (s, 4 H), 4.82 (d, 4 H, J_{H-H} = 11 Hz), 8.54 (s, 1 H). ^{13}C{^{1}H} NMR (100 MHz, toluene-d_8, 27 °C): δ 0.00 (s, $SiMe_3$), 28.69 (s, $C(CH_3)_3$), 29.47 (s, $C(CH_3)_3$), 29.72 (s, $C(CH_3)_3$), 35.67 (s, CH_2), 36.14 (s, CH_2), 36.50 (s, CH_2), 81.05 (s, $C(CH_3)_3$, 85.38 (s, $C(CH_3)_3$, 88.56 (s, $C(CH_3)_3$, 166.50 (s, $NNC(H)SiMe_3$). IR (ν_{max}/cm^{-1}): 1477 (s), 1463 (vs), 1419(vw), 1392 (s), 1377 (s), 1363 (s), 1372 (s), 1301 (vw), 1289 (vw), 1260 (w), 1250 (m), 1217 (w), 1058 (vs), 1031 (s), 1022 (vs), 1005 (vs), 994 (s), 932 (m), 905 (w), 864 (m), 845 (m), 805 (w), 754 (m), 721 (w), 690 (s), 680 (s), 658 (s), 639 (m), 600 (m), 577 (w), 492 (vw), 458 (m), 436 (vw), 403 (m), 375 (s). UV-vis (THF, λ_{max}/nm): 475 (ε/dm^3 mol^{-1} cm^{-1} = 300), 268 (37,000), 255 (74,000), 249 (64,000) 244 (52,000), 239 (40,000), 234 (30,000). Anal. Calc. for $W_2N_2O_8C_{44}H_{98}$: C, 44.82; H, 8.39; N, 2.38. Found: C, 44.72; H, 8.39; N, 2.32%.

Electronic structure calculations

Density functional theory (DFT) calculations with the Gaussian 98 suite of programs[13] utilized the B3LYP[14–16] method and standard basis sets. C, H, O, and N were described with the 6-31G* basis set (and 5 "pure" d functions), while W[17] was represented by an SDD effective core potential. The geometries were optimized under C_1 symmetry starting from the solid-state structure coordinates using the default optimization criteria. Methoxide ligands were substituted for neopentoxides. Stationary points were characterized as minima by vibrational frequency calculations.

Crystallographic studies

$W_2(\mu\text{-}N_2C(H)SiMe_3)(\mu\text{-}OCH_2{}^tBu)_2(OCH_2{}^tBu)_6$. The data collection crystal was an amber colored, triangular plate. Examination of the diffraction pattern on a Nonius Kappa CCD diffractometer indicated a triclinic crystal system. All work was done at 200 K using an Oxford Cryosystems Cryostream Cooler. The data collection strategy was set up to measure a hemisphere of reciprocal space with a redundancy factor of 3, which means that 90% of the reflections were measured at least 3 times. A combination of ϕ and ω scans with a frame width of 1.0° was used. Data integration was done with Denzo.[18] Scaling and merging of the data were done with Scalepack;[18] application of an absorption correction is inherent in this treatment and is reflected in the scale factor range of 9.14 to 12.56. Merging the data and averaging the symmetry equivalent reflections results in an R(int) value of 0.051. The teXsan[19] package indicated the space group to be $P\bar{1}$ based on the intensity statistics.

The positions of the two W atoms were determined by the Patterson method in SHELXS-86.[20] The rest of the non-hydrogen atoms were located by a combination of DIRDIF[21] and standard Fourier methods. Full-matrix least-squares refinements based on F^2 were performed in SHELXL-93.[22]

For both structures, the methyl group hydrogen atoms were added at calculated positions using a riding model with U(H) = 1.5 × U_{eq}(bonded C atom). For each methyl group, the torsion angle which defines its orientation about the Si–C or C–C bond was refined. The other hydrogen atoms were included in the model at calculated positions using a riding model with U(H) = 1.2 × U_{eq}(bonded C atom). Neutral atom scattering factors were used and include terms for anomalous dispersion.[23] Crystallographic details of both structures are in Table 3.

$W_2(\mu\text{-}NPh)(\mu\text{-}OCH_2{}^tBu)_2(OCH_2{}^tBu)_6\cdot$½hexane. The data collection crystal was an orange-red rectangular rod. Examination of the diffraction pattern on a Nonius Kappa CCD diffractometer indicated a triclinic crystal system. All work was done at 200 K using an Oxford Cryosystems Cryostream Cooler. The data collection strategy was set up to measure a hemisphere of reciprocal space with a redundancy factor of 2.7, which means that 90% of the reflections were measured at least 2.7 times. A combination of ϕ and ω scans with a frame width of 1.0° was used. Data integration was done with Denzo.[18] Scaling and merging of the data were done with Scalepack;[18] application of an absorption correction is inherent in this treatment and is reflected in the scale factor range of 9.41–12.39. Merging the data and averaging the symmetry equivalent reflections resulted in an R(int) value of 0.046. The teXsan[19] package indicated the space group to be $P\bar{1}$ based on the intensity statistics.

The structure was solved by the Patterson method in SHELXS-86.[20] Besides the W complex, the asymmetric unit contains a hexane molecule positioned on an inversion center. Full-matrix least-squares refinements based on F^2 were performed in SHELXL-93.[22] The hexane molecule was refined isotropically, and only the hydrogen atoms bonded to the CH_2 groups were included in the model.

CCDC reference numbers 192252 and 192253.

Table 3 Crystallographic details

	$W_2(\mu\text{-}N_2C(H)SiMe_3)(\mu\text{-}OCH_2{}^tBu)_2(OCH_2{}^tBu)_6$	$W_2(\mu\text{-}NPh)(\mu\text{-}OCH_2{}^tBu)_2(OCH_2{}^tBu)_6\cdot$½hexane
Empirical formula	$C_{44}H_{98}N_2O_8SiW_2$	$C_{46}H_{93}NO_8W_2$ + ½ hexane
Formula weight	1179.03	1199.00
Temperature/K	200	200(2)
Wavelength/Å	0.71073	0.71073
Crystal system	Triclinic	Triclinic
Space group	$P\bar{1}$	$P\bar{1}$
a/Å	11.921(1)	12.030(1)
b/Å	11.954(1)	12.048(1)
c/Å	21.526(2)	20.567(2)
a/°	88.91(1)	92.84(1)
β/°	85.00(1)	99.67(1)
γ/°	74.92(1)	102.96(1)
Volume/Å^3	2950.6(5)	2851.9(5)
Z	2	2
D_c/Mg m^{-3}	1.327	1.396
Absorption coefficient/mm^{-1}	3.957	4.075
F(000)	1204	1226
Crystal size/mm	0.15 × 0.31 × 0.42	0.08 × 0.15 × 0.31
Reflections collected	79939	63505
Independent reflections	13454 [*R*(int) = 0.051]	13080 [*R*(int) = 0.046]
Goodness-of-fit on F^2	1.034	1.092
Final *R* indices [$I>2\sigma(I)$][a]	$R1 = 0.0263$, $wR2 = 0.0578$	$R1 = 0.0295$, $wR2 = 0.0569$
R indices (all data)	$R1 = 0.0421$, $wR2 = 0.0621$	$R1 = 0.0481$, $wR2 = 0.0613$
Largest diff. peak and hole/e Å^{-3}	1.46 and −0.84	1.43 and −1.01

[a] $R1 = \Sigma||F_o| - |F_c||/\Sigma|F_o|$ and $wR2 = [\Sigma w(F_o^2 - F_c^2)^2/\Sigma w(F_o^2)^2]^{1/2}$.

See http://www.rsc.org/suppdata/dt/b3/b304587k/ for crystallographic data in CIF or other electronic format.

Acknowledgements

We thank the National Science Foundation for financial support and The Ohio Supercomputing Center for computational resources.

References

1 F. A. Cotton and R. A. Walton, *Multiple Bonds Between Metal Atoms*, Oxford University Press, Oxford, 2nd edn, 1993.
2 B. G. Brandt and A. G. Skapski, *Acta. Crystallogr.*, 1966, **21**, 482.
3 T. A. Budzichowski, M. H. Chisholm, K. Folting and W. E. Streib, *J. Am. Chem. Soc.*, 1995, **117**, 7429.
4 (*a*) M. H. Chisholm, K. Folting, M. A. Lynn, W. E. Streib and D. B. Tiedtke, *Angew. Chem., Int, Ed. Engl.*, 1997, **37**, 52; (*b*) M. H. Chisholm, W. E. Streib, T. B. Tiedtke and D. D. Wu, *Chem. Eur. J.*, 1998, **4**, 1470.
5 M. H. Chisholm, D. R. Click, C. M. Hadad and J. C. Gallucci, *J. Chem. Soc., Dalton Trans.*, 2001, 2074.
6 (*a*) A. J. Nielson, J. M. Waters and D. C. Bradley, *Polyhedron*, 1983, **2**, 285; (*b*) A. J. Nielson and J. M. Waters, *Polyhedron*, 1982, **1**, 151; (*c*) D. C. Bradley, A. J. Nielson, M. B. Hursthouse and J. D. Runnades, *Polyhedron*, 1991, **10**, 477; (*d*) A. A. Danopoulus, G. Wilkinson, B. Hussain-Bates and M. B. Hursthouse, *J. Chem. Soc. Dalton Trans.*, 1987, 2059.
7 F. A. Cotton, S. A. Duraj and W. Roth, *J. Am. Chem. Soc.*, 1984, **105**, 4749.
8 (*a*) L. Messerle and M. D. Curtis, *J. Am. Chem. Soc.*, 1982, **104**, 1537; (*b*) L. Messerle and M. D. Curtis, *Organometallics*, 1987, **6**, 1713; (*c*) L. Messerle and M. D. Curtis, *J. Am. Chem. Soc.*, 1980, **102**, 7789; (*d*) M. H. Chisholm, K. Folting, J. C. Huffman and A. L. Ratermann, *Inorg. Chem.*, 1984, **23**, 2303.
9 (*a*) W. A. Herrmann, C. Kruger, R. Goddard and I. Bernal, *Angew. Chem., Int. Ed. Engl.*, 1977, **16**, 334; (*b*) A. D. Clauss, P. A. Dimas and J. R. Shapley, *J. Organomet. Chem.*, 1980, **201**, 631; (*c*) M. Green, R. M. Mills, G. N. Pain, F. G. A. Stone and P. M. Woodward, *J. Chem. Soc., Dalton Trans.*, 1982, 1309.
10 (*a*) A. Zanotti-Gerosa, E. Solari, L. Giannisi, C. Floriani, A. Chiesi-Villa and C. Rizzoh, *J. Am. Chem. Soc.*, 1998, **120**, 437; (*b*) G. Guillemot, E. Solari, R. Scopelliti and C. Floriani, *Organometallics*, 2001, **20**, 2446.
11 F. Maseras, M. A. Lockwood, O. Eisenstein and I. P. Rothwell, *J. Am. Chem. Soc.*, 1998, **120**, 6598.
12 H. Schaefer, W. Saak and M. Weidenbruch, *Organometallics*, 1999, **18**, 3159.
13 M. J. Frisch, G. W. Trucks, H. B. Schlegel, G. E. Scuseria, M. A. Robb, J. R. Cheeseman, V. G. Zakrzewski, J. A. J. Montgomery, R. E. Stratmann, J. C. Burant, S. Dapprich, J. M. Millam, A. D. Daniels, K. N. Kudin, M. C. Strain, O. Farkas, J. Tomasi, V. Barone, M. Cossi, R. Cammi, B. Menuucci, C. Pomelli, C. Adamo, S. Clifford, J. Ochterski, G. A. Pertersson, P. Y. Ayala, Q. Cui, K. Morokuma, D. K. Malick, A. D. Rabuck, K. Raghavachari, J. B. Foresman, J. Cioslowski, J. V. Ortiz, A. G. Baboul, B. B. Stefanov, G. Liu, A. Liashenko, P. Piskorz, I. Komaromi, R. J. Gomperts, R. L. Martin, D. J. Fox, T. Keith, M. A. Al-Lahman, C. Y. Peng, A. Nanayakkara, M. Challacombe, P. M. W. Gill, B. Johnson, W. Chen, M. W. Wong, J. L. Andres, C. Gonzalez, M. Head-Gordon, E. S. Replogle and J. A. Pople, Gaussian 98 Version A9, Gaussian Inc., Pittsburgh, PA, 1998.
14 A. D. Becke, *Phys. Rev. A*, 1988, **38**, 3098.
15 A. D. Becke, *J. Chem. Phys.*, 1993, **98**, 5648.
16 C. Lee, W. R. Yang and G. Parr, *Phys. Rev. B*, 1988, **37**, 785.
17 D. Andrae, U. Haeussermann, M. Dolg and H. Stoll, *Theor. Chim. Acta*, 1990, **77**, 123.
18 DENZO, Z. Otwinowski and W. Minor, *Methods in Enzymology, Macromolecular Crystallography, Part A*, ed. C. W. Carter, Jr. and R. M. Sweet, Academic Press, New York, 1997, vol. 276, 307–326.
19 teXsan, Crystal Structure Analysis Package, version 1.7–2, Molecular Structure Corporation, The Woodlands, TX, 1995.
20 SHELXS-86, G. M. Sheldrick, *Acta Crystallogr., Sect. A*, 1990, **46**, 467.
21 V. Parthasarathi, P. T. Beurskens and H. J. B. Slot, *Acta Crystallogr., Sect. A*, 1983, **39**, 860.
22 G. M. Sheldrick, SHELXL-93, University of Göttingen, Germany, 1993.
23 *International Tables for Crystallography*, Kluwer Academic Publishers, Dordrecht, 1992, vol. C.
24 M. N. Burnett and C. K. Johnson, ORTEP-III, Oak Ridge Thermal Ellipsoid Plot Program for Crystal Structure Illustrations, Report ORNL-6895, Oak Ridge National Laboratory, Oak Ridge, TN, USA, 1996.